

Data analyses

SWR extraction and SWR single unit modulation. Sharp wave ripples (SWR) are periods of abrupt depolarization at a frequency of 150-250Hz, accompanied by hippocampal spike bursts, periods of increased hippocampal spiking activity. We extracted periods of immobility on the behavioral apparatus (speed lower than 4 cm/sec), and computed the Hilbert transform of the band-pass filtered HIPP LFP (150-250Hz), smoothed with a 50ms moving-average window. We binned hippocampal multi-unit activity at 20ms. From these data we collected those time points in which LFP and MUA z-scores passed a threshold of 3 (Supplementary Figure S1). For events closer than 500ms we collected only the first event. Spikes from each single unit occurring within +/-500ms of a ripple onset were binned at 100ms. Statistical assessment of single-unit ripple modulation was done using a Kruskal-Wallis ANOVA (followed by post-hoc comparisons) on 10 non-overlapping 100ms bins surrounding (+/- 500ms) the ripple onset. To estimate the beginning of SWR we determined the time point at which hippocampus exhibits significant increases in LFP power at ripple frequency, and in the 5ms-binned MUA firing rate. We thus gathered all MUA and LFP vectors corresponding to all SWR events, and used Kruskal-Wallis ANOVA (followed by post-hoc comparisons) to compare such activity measurements between time bins +/-500ms of SWR detection points. We repeated this analysis for cingulate cortical data to compare the SWR initiation in HIPP with the earliest significant change in MUA and LFP of cingulate data. This allowed us to determine, on average, the temporal lapse between HIPP SWR and statistically significant increases in cortical activity.

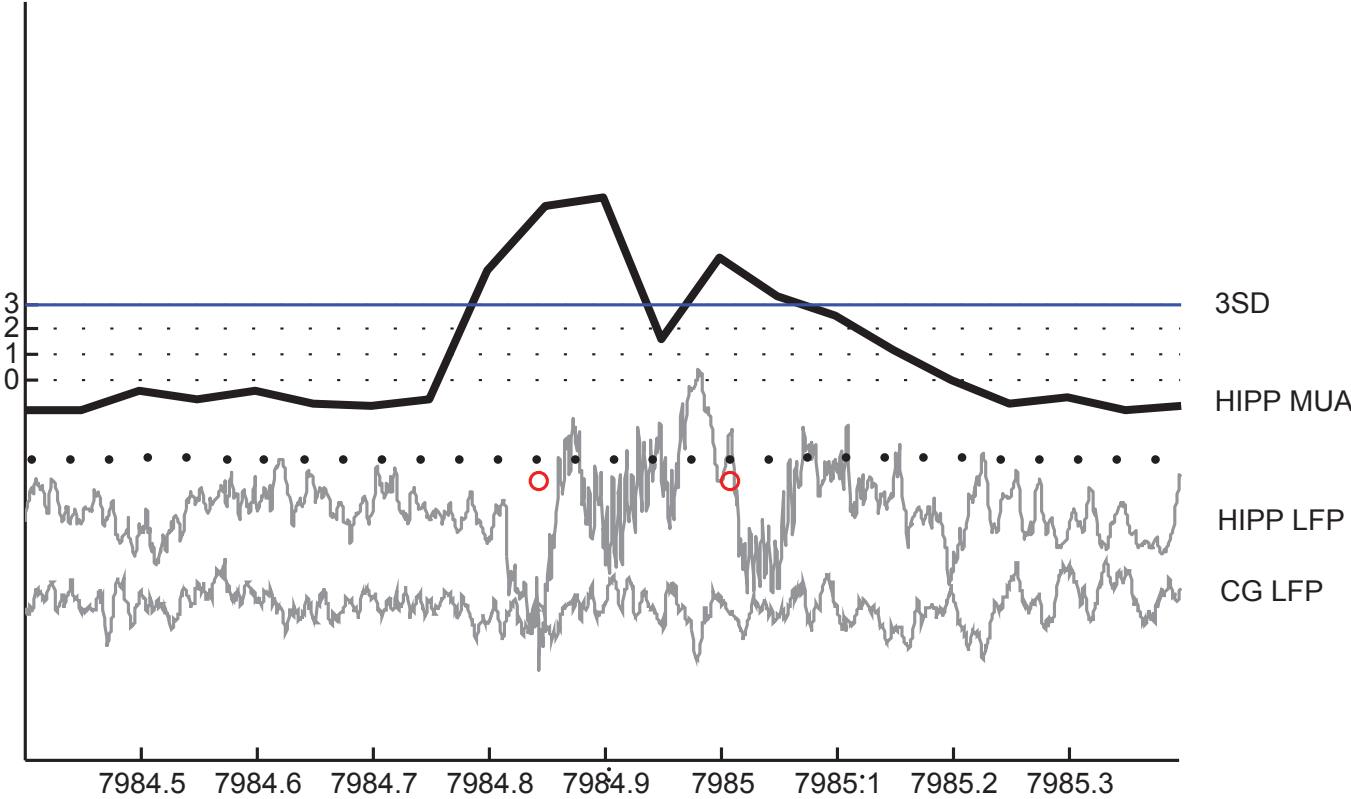
CG-HIPP LFP coherence during SWR. Raw CG and HIPP LFP, and 5ms-binned multi-unit spikes (MUA), +/-500ms of SWR were used to compute coherence and spectra on 250ms windows sliding by 10ms. We then corrected these values for a baseline of 250ms just preceding the SWR detection point, tested for differences in the magnitude of baseline-corrected coherence, at all frequencies up to ~82Hz (high- γ), between consecutive non-overlapping 250ms bins (Kruskal Wallis ANOVA followed by multiple comparisons), as well as between the 250ms before (the pre-SWR baseline) and the 250ms after HIPP SWR, (Wilcoxon Sign Test). Instantaneous frequency was computed by extracting, from each dataset, the inverse of the inter-peak interval of the wide-band γ LFP (10-80Hz) from CG and HIPP, and plotting this value's *pdf* across all datasets. For LFP phase-offset analyses, phases were extracted from the slow- γ LFP (filtered at 23-30Hz) from which SWR-triggered CG-to-HIPP phase offset (ϕ) was computed. CG-HIPP phase-locking was computed as the circular concentration (κ) of CG-HIPP ϕ , at 250ms bins before and after SWR, corrected for the value corresponding to the same pre-SWR baseline period (250ms preceding SWR). Differences in the average γ -phase offset Kappa between pre- and post-SWR 250ms bins were assessed as before.

Single unit SWR modulation. In order to get a measure of the degree to which each single units' firing rate is changed during hippocampal SWR, we computed the difference between the firing rate in the 100ms time bin before, and the one after the SWR, divided by the mean rate during wakefulness: $\Delta_{SWR} = abs(\delta_{before} - \delta_{after}) / \delta_{avg}$ (Supplementary Figure S2).

Single unit HIPP LFP γ modulation. Individual CG spike phases were extracted for each dataset and single unit. Each CG single unit's γ phase modulation was computed as the

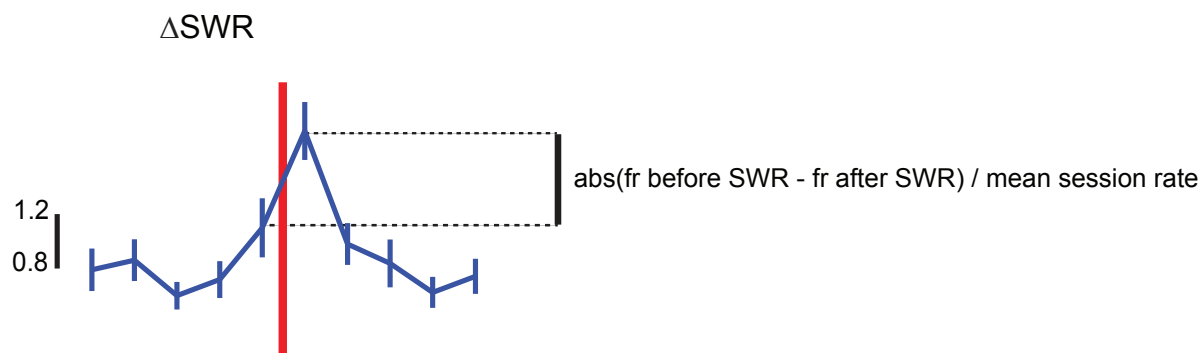
circular concentration (κ) of the distributions of slow- γ phases (of the HIPP LFP filtered between 23-30 Hz) pertaining to each of the behavioral modes considered: active running, immobility during wakefulness excluding SWR, and SWR events (in consecutive, non-overlapping 250ms bins). Differences in mean Kappa between 250ms bins surrounding SWR were tested using Kruskal-Wallis ANOVA, followed by post-hoc comparisons.

Correlations. Correlations between CG single units' phase and SWR modulations were computed using Spearman correlation and partial-correlation coefficients. To ascertain frequency specificity, we repeated these analyses for the frequency range below (β 15-21Hz), and above (high- γ 50-80Hz).



Remondes Supplementary Figure S1 - related to Figure 1

Graphic representation of SWR extraction, immobility wakefulness periods during which MUA and filtered LFP crossed 3SD.



Remondes Supplementary Figure S2 - related to Figure 4

Δ SWR is computed by taking the difference between the firing rate (fr) in the 100ms before the SWR and the one 100ms after the SWR, normalized by the average rate during wakefulness.